Antiplasmodial biodereplication based on highly efficient methods

Pedro G. Vásquez-Ocmín[†], Jean-François Gallard[‡], Anne-Cécile Van Baelen[†], Karine Leblanc[†], Sandrine Cojean[†], Elizabeth Mouray[‖], Philippe Grellier[‖], Carlos Amasifuén[⊥], Guillaume Bernadat[†], Laurent Evanno[†], Bruno Figadère[†], Alexandre Maciuk[†*].

[†] Université Paris-Saclay, CNRS, BioCIS, 92290, Châtenay-Malabry, France.

[‡]Institut de Chimie des Substances Naturelles CNRS UPR 2301, Université Paris-Saclay, 1 Avenue de la Terrasse, 91198 Gif-sur-Yvette, France

[‖] Unité Molécules de Communication et Adaptation des Microorganismes (MCAM, UMR 7245), Muséum National d'Histoire Naturelle, CNRS, Sorbonne Universités, CP52, 57 Rue Cuvier, 75005 Paris, France

[⊥]Universidad Nacional Toribio Rodríguez de Mendoza de Amazonas, Facultad de Ingeniería Civil y Ambiental, Chachapoyas, Perú

*alexandre.maciuk@u-psud.fr

ABSTRACT:

Research on malaria remains mandatory to explain the biochemistry and biology of *Plasmodium* parasite. In spite of its several drawbacks, natural products research regularly proves to be one of the main tools to fight malaria. Smart screening strategies are necessary to hasten this process. We propose a biodereplication method using mass spectrometry and combining the classical dereplication approach with the predominant mechanism of action of antimalarial drugs. The method encompasses a biomimetic heme binding assay (heme adducts detection by MS), molecular networking for quick data mining, CPC for extract fractionation and compounds isolation and *in silico* modeling of heme adducts by molecular docking. This method has been applied to the Amazonian medicinal plant *Piper coruscans* (Piperaceae). Twelve targeted compounds were isolated, principally phenolic compounds accounting for the *in vitro* biological activity of *P. coruscans* extract.

Keywords: Biodereplication, *Plasmodium falciparum*, heme, mass spectrometry, biomimetic.

INTRODUCTION

Malaria is an infectious disease caused by four protozoan species of the genus *Plasmodium* (*P. falciparum*, *P. malariae*, *P. ovale,* and *P. vivax*).[1] The most widespread and severe form of the disease is caused by *P. falciparum*, which transiently infects the liver before invading red blood cells of the mammalian host. Clinical manifestations occur during the erythrocytic stage and can include fever, chills, headache, muscular aching and weakness, vomiting, cough, diarrhea and abdominal pain, generalized convulsions, circulatory collapse and can be followed by coma and death if not treated. Initial symptoms, sometimes of mild intensity, may not be easy to recognize as being due to malaria.[2] Malaria is commonly associated with poverty, but is also a cause of poverty and a major hindrance to economic development. For decades compounds derived from chloroquine and now artemisinin have been used in combination with other drugs to fight malaria.[3] Nevertheless, *Plasmodium*'s ever-growing resistance to these medicines continues to make it a global health problem.[4,5] A major factor that severely hinders the efforts to 'roll back malaria' is the emergence and spread of parasites resistant to affordable antimalarial agents.[6] Research of novel antimalarial molecules involves, in a general way, the screening of compounds obtained by medicinal or combinatorial chemistry or isolated from Nature, followed by improvement of these molecules by hemisynthesis to enhance biological activity. Bioguided isolation of natural products from complex extracts is ambiguous, because the mechanism of action is not known a *priori*, so complementary tests are needed. Owing to the considerable progresses of compounds isolation and identification made during the past decades, combination of chemical and computational tools currently allow to "dereplicate" an extract whatever the origin (vegetal, marine organism, microbial, etc.) with the purpose to discard known, mildly active molecules.[7] Historically, the first definition of the term ''dereplication'' was given by Beutler et al. in 1990 as ''a process of quickly identifying known chemotypes".[8] Today one stunningly performant example of dereplication is molecular networking (MN), a computer-based approach allowing to visualize and organize tandem mass spectrometry datasets and to automate database search for metabolite

identification within complex mixtures.[9] Such a tool relies on the observation that structurally similar metabolites share similar MS-MS fragmentation patterns.[10,11] Dereplication approaches *strictu senso* do not unequivocally identify compounds but annotate them as being identical to a known compound with a high probability. Such approaches also do not give any biological information. We propose the term "biodereplication", as the early detection in a complex mixture of compounds responsible for the activity, before any isolation or formal identification.

Mechanism of action of quinoline drugs like chloroquine is based on the inhibition of the crystallization pathway of free heme, which is released inside the *Plasmodium* digestive vacuole (PDV) after hemoglobin proteolysis.[12] The PDV is a multiphasic mixture of neutral lipids in the form of nanospheres suspended in an aqueous solution of proteins, at a pH ranging from 4.8 to 5.5[13–15]. It is an acidic proteolytic compartment crucial for the metabolism of the parasite. In this vacuole, amino acids are transported, oxygen radicals are detoxified, drugs are accumulated, acidification is maintained and free iron is generated.[16] Due to the important roles of heme in elementary cellular processes of most organisms and especially in *Plasmodium*, heme metabolism is historically a major target for anti-parasitic drug, and is still considered as a promising target for new molecules.[17–19] Understanding heme crystallization process has been a pivotal point in characterizing the mechanism(s) of action of the major quinoline antimalarial drugs[20], and crucial for the development of new drugs able to overcome parasite resistance.[21] Formation of π-π non-covalent bounds is a necessary requirement for the inhibition of heme crystallization by antimalarial drugs.[22,23] Muñoz-Durango *et al*[24] work was taken as starting point with the aim to optimize the biological conditions and mimic the multiphasic and acidic conditions of PDV. Isolation of potentially active molecules guided by biodereplication on heme binding assay were isolated from an extract of *Piper coruscans* Kunth (Piperaceae).

EXPERIMENTAL SECTION

1. Heme-binding assay by MS.

Hemin (iron-containing porphyrin with chlorine counterion) and crude ethanolic extract were dissolved in DMSO at 5 mM and 10 mg/mL, respectively. Pure

compounds were dissolved in DMSO at the concentration of 10 mM, excepted Tween 20 which was dissolved in water at 10 µM. Citric buffer saturated octanol (CBSO)[25] was prepared by mixing 5 mL of citric acid 50 mM pH 5.2 and 15 mL of n-octanol (anhydrous, ≥99%) and letting it to settle at 23 °C for 30 min. Upper phase of CBSO was used. Autosampler 1260 infinity G1367E 1260 Hip ALS (Agilent Technologies) was used to do the automatic mixing of aliquots in a 384-well plates. Incubation mixture was as follows: compound 5 µL + heme 5 µL + Tween 5 µL + organic phase of CBSO 85 µL. Samples were injected in infusion mode (direct injection) in a 6530 Accurate-Mass QToF LC/MS instrument (Agilent Technologies) with the following settings: positive ESI mode, 2 GHz acquisition rate. Ionization source conditions were: drying gas temperature 325 °C, drying gas flow rate 11 L/min, nebulizer 35 psig, fragmentor 175 V, skimmer 65 V. Range of *m/z* was 200-1700. In the positive-ion mode, purine $C_5H_4N_4$ $[M + H]^+$ ion (*m/z* 121.050873) and the hexakis (1 H,1H,3H-tetrafluoropropoxy)-phosphazene $C_{18}H_{18}F_{24}N_3O_6P_3$ $[M+H]^+$ ion (*m/z* 922.009 798) were used as internal lock masses. Full scans were acquired at a resolution of 11 000 (at m/z 922).

On the same spectrum (spectral windows) appears heme at *m/z* 616.16; adducts at *m/z* 616.16 + "X" and 2heme + "X"; heme + DMSO *at m/z* 694.19; heme dimers at *m/z* 1231.32 $[2heme - H]^+$; *m/z* 1253.30 $[2heme - 2H + Na]^+$; *m/z* 1267.26 $[2heme + {}^{35}Cl]^+$ and 1269.24 $[2heme + {}^{37}Cl]^+$. Chloroquine 5 mM in water (chloroquine diphosphate, Sigma-Aldrich) and artemisinin (Sigma-Aldrich) were used as positive control. To obtain heme-Fe(II) from hemin (heme-Fe(III)), glutathion (50 mM in water) was mixed with hemin (5 mM in DMSO) in a ratio 1:1 and let to incubate 40 min. This solution was used as heme solution as described above.

2. Visualization of adducts fragmentation by molecular networking (MN)

Ethanolic extract and hemin (heme-Fe(III)) were mixed and injected using infusion mode for MSMS experiment. Three collision energies were used: 30, 50, and 70 eV. Ten most intense ions (Top 10) per cycle were selected. MSMS acquisition parameters were as follows: *m/z* range 100-1700, default charge of 1, minimum intensity of 5000 counts, 3 spectra/s, isolation width: narrow mode (1.3 *m/z*). A list of compounds was generated by the

"find by auto MSMS" algorithm of MassHunter software (Qualitative Analysis B.07.00, Agilent Technologies). The mode "extract average MSMS spectrum" was used to sum up and average the results of the 3 collision energies. Exportation of generated spectra was made in MGF format using the option "entire data file". Information generated were uploaded onto the online platform GNPS (global natural product social network).[26] Parameters used for the algorithm were: precursor ion mass tolerance = 1; fragment ion mass tolerance = 0.3; min pairs cos = 0.7; minimum matched fragment ions = 3; minimum cluster size = 1. From the data a network was calculated measuring correlations and plotted using Cytoscape 3.5.1. Each *m/z* of adducts [heme + "X"]$^+$ was observed as an individual node in the same cluster, related to each other in agreement with the loss of a similar fragment (heme at *m/z* 616.16). An alkaloid extract from *Cinchona pubescens* Vahl (Rubiaceae) and eight antiplasmodial drugs (chloroquine, quinine, amodiaquine, ketoconazole, miconazole, mefloquine, praziquantel, sulfadoxine) were used as examples of visualization of adducts fragments by MN. Methodology and conditions were the same as described above.

3. Collision induced dissociation

Dissociation in the collision chamber was caused by increasing collision energies from 0 to 56 eV. MSMS targeted mode, isolation width of *m/z* 1.3 and flow injections analyses (FIA) were used. MSMS parameters were the same as described above. Results were plotted and the sigmoidal regression curve could allow to calculate the energy necessary to dissociate 50 % of adducts (DV_{50}) using GraphPrism or Python.[24]

4. Biological material

Leaves of *Piper coruscans* Kunth (Piperaceae) were collected in December 2016 in Lupuna (Zona II) village, in the province of Maynas, located in the region of Loreto, Peru (18M 0704173, UTM 9585656). The plant was identified by Dr. Carlos Amasifuén and deposited at the National Herbarium of the San Marcos University, Lima, Peru. Leaves dried and ground (600 g) were soaked 24 h twice in 5 L of ethanol 96%, filtrated and the extract evaporated under reduced pressure, below 40 °C.

5. Isolation of targeted compounds.

Molecules isolation were performed using centrifugal partition chromatography (CPC) (Sanki LLB-M, 200 ml capacity), preparative HPLC and LCMS. Liquid-liquid extraction was carried out on 60 g of ethanolic extract using cyclohexane/water with cyclohexane (PCC fraction) yielding 45 g, ethyl acetate/water with ethyl acetate (PCA fraction) yielding 10g and water (PCAq fraction) yielding 11g. Targeted molecules were localized by means of LC-MS analysis in the cyclohexane and ethyl acetate extracts. CPC in descending mode was performed on 1.8 g of PCC fraction using the biphasic solvents system heptane/ethyl acetate/butanol/methanol/water (20:10:10:30:30) determined by testing several biphasic systems and analyzing both phases by LCMS. Fractions of 0.5 mL were collected, analyzed by LCMS and grouped into 15 sub-fractions. Isolated compounds were aurentiacin, compound **1** (20 mg); strobopinin 7-methyl ether, **4** (18 mg); and 5-hydroxy-7-methoxy-6,8-dimethyl flavanone, **5** (7 mg).Then, CPC in descending mode was performed from 8 g of PCA fraction using the biphasic solvents system heptane/ethyl acetate/butanol/methanol/water (12:14:14:23:37) determined by testing several biphasic systems and analyzing both phases by LCMS, with similar conditions described above. Six sub-fractions were obtained, including PCA-2 (yielding 840 mg). A second CPC in descending mode was performed on 800 mg of PCA-2 with heptane/ethyl acetate/butanol/methanol/water (8:16:16:18:42), giving 13 sub-fractions. Preparative HPLC was performed on a Sunfire column C18, 4.6 x 150 mm – 5µm (Waters) as stationary phase and water (0.1 % formic acid)/acetonitrile (30 to 70 % in 20 minutes) as mobile phase. Eight compounds were isolated: desmethoxymatteucinol, **6** (1.2 mg); 2', 4'-dihydroxy-6'-methoxy-3'-methylchalcone, **2** (0.8 mg); cardamomin, **3** (3.7 mg); alpinetin, **7** (1.1 mg); compound **10** (1.3 mg); pinocembrin, **8** (2.6 mg); dimethyl cryptostrobin, **9** (0.6 mg), *N*-benzoyltyramine methyl ether, **11** (1.9 mg). Along with these targeted compounds one untargeted compound was isolated: 1*H*-inden-1-one, **12** (3 mg). Details of compounds identification and NMR spectroscopic data are given in supplementary information (see SI1-SI4).

6. Antiplasmodial activity

Plasmodium falciparum culture

The chloroquine-sensitive 3D7 *P. falciparum* strain (clone of the NF54) was obtained from Malaria French National Reference Center (CNR Paludisme, Hôpital Bichat Claude Bernard, Paris). The strains were maintained in O^+ human erythrocytes in albumin supplemented RPMI medium under continuous culture using the candle-jar method.[27] The parasites were synchronized to the ring stage by repeated sorbitol treatment.[28]

In vitro antiplasmodial activity on *Plasmodium falciparum*.

A 2.5% (V/V) erythrocytes suspension with 1 % parasitemia (number of infected red blood cells per 100 red blood cells) was incubated in duplicates with the compounds at concentrations ranging from 48.5 nM to 100 µM, obtained by serial dilution. After 44 h of incubation at 37 °C, the plates were subjected to 3 freeze-thaw cycles to achieve complete hemolysis. The parasite lysis suspension was diluted 1:5 in lysis buffer. *In vitro* susceptibility is expressed as the concentration inhibiting 50 % of the parasite's growth (IC_{50}). Parasite growth was determined by using SYBR® Green I, a dye with strong fluorescence enhancement upon contact with DNA. Incorporation of SYBR® Green I (Applied Biosystems, France) in parasite DNA was measured using the Master epRealplex cycler® (Eppendorf, France) according to the following program to increase the SYBR® Green I incorporation: 90 °C (1 min), decrease to 10 °C over 5 min followed by fluorescence reading. Untreated infected and uninfected erythrocytes were used as controls and chloroquine diphosphate (Sigma, France) as reference drug.[29,30] IC_{50} was calculated by IC-estimator online software (http://www.antimalarial-icestimator.net).

7. Cytotoxicity studies

Cellular cytotoxicity was evaluated using the AB943 primary human dermal fibroblast cell line maintained at 37 °C in RPMI 1640 medium supplemented with 10% (v/v) fetal calf serum. Cells were seeded in 96-well plates (20,000 cells/mL) and incubated for 24 h, then treated with the drug for 72 h. After incubation, the cell growth medium was replaced by 100 µL RPMI 1640 containing 20% (v/v) Alamar Blue (Thermo-Fisher, France). Fluorescent viable cells were monitored after 5 h of incubation at 37 °C, at a wavelength of 530

nm for excitation and 590 nm for emission, in a FL600 luminescence spectrometer (Biotek, France). CC_{50}, corresponding to drug concentrations causing 50% of AB943 cell proliferation inhibition, were calculated from the drug concentration-response curves.[31]

8. *ADMET Prediction*

ChemSketch (ACD/Labs Products) software was used to screen all compounds in order to predict their lipophilicity. The input file were previously generated as SK2 files and prediction of logP were estimated.[32]

9. Molecular Docking

Starting coordinates of heme and compound were obtained by minimization using a molecular mechanics force field implemented by MarvinSketch v17.28 software package [www.chemaxon.com]. Resulting structure of compounds xx were then docked against heme using AutoDock Vina 1.1.2 software package.[33] Depiction of the highest ranked solution was performed using UCSF Chimera v1.11 software package.[34]

RESULTS AND DISCUSSION

Heme (ferriprotoporphyrin IX-Fe(III)PPIX) is an ubiquitous and essential molecule which plays key biological roles in processes like oxygen transport, respiration, photosynthesis and drug detoxification.[35,36] Free heme is a strong oxidizing agent and sequestration of heme into hemozoin (first through heme aggregates and then into actual crystals) is a suitable target for new antimalarial drugs, which has been referred to as the "Achilles heel of the parasite".[37,38] Different chemical and physical factors modulate hemozoin formation, such as the degree of hydrophobicity of native, surrounding alcohols and lipids in the digestive vacuole, their ability to solubilize heme aggregates or reduce surface tension. *In vitro* experiments showing also that increasing physical contact between heme aggregates by stirring increases this formation.[39] So far, several methodologies were used for the detection of adducts heme-compounds in the drug discovery line, *i.e.*, classical spectrophotometric microassay of heme polymerization (HPIA)[22,40], nuclear magnetic resonance (NMR)[41] or mass spectroscopy (MS) by electrospray ionization.[24,42] In our view, detection of covalent and non-covalent

adducts by MS is the most effective means, ensuring the annotation of the exact molecular mass of adduct.

First reports on the monitoring by MS of non-covalent complexes appeared in the literature in the early 1990s, with initial studies focusing on protein-ligand complexes quickly joined by studies in which protein-protein interactions were maintained.[43] Indeed ESI provides a rapid, sensitive and highly selective tool for probing non-covalent interactions.[44,45] Moreover it is a gentle ionization method, yielding no molecular fragmentation and allowing intact weakly bound complexes to be detected.[43] Noteworthy, collision-induced dissociation (CID) can be induced in the so-called "fragmentor" zone of Agilent instruments (or in the equivalent zone in instruments of other manufacturers), which is technically the atmospheric pressure/vacuum interface. Such CID can be performed on single MS instruments, but is not finely tunable. Provided the fragmentor voltage is kept at a low value, stable non-covalent complexes can be formed between Fe(III)-heme and antimalarial agents, *i.e.*, quinine, artemisinin and its derivatives dihydroartemisinin, α- and β-artemether, and arteether.[12] Binding strengths between drugs and Fe (III)-heme can also assessed in a relative mode. This approach has previously been shown to be useful in determining the structure-activity relationship of antimalarial agents, namely, terpene isonitriles and neocryptolepine derivatives.[46] So far this approach has mainly be used to assess the strength of π-π non-covalent binding.[24,42,47] In this work we "biodereplicated" an ethanolic extract, addressing the main mechanism of action of antimalarial drugs like quinoleins. We combined information generated by Q-ToF MS (non-covalent adducts identification) and MS-MS (analysis of the fragmentation pathway by MN) to determine potentially active compounds independently of their chemical structures.

In this study**,** a miniaturized and automated methodology was developed which improves the methodology described by Muñoz-Durango *et al*,[24] to allow high-throughput screening format and reduce false positives. The overall workflow is presented in **Figure 1**. It mimics the pH (5.2) as well as the multiphasic conditions (aqueous-lipid interface) of the PDV.[37] In order to achieve this, three criteria had to be fulfilled: 1) the solution formed must have a pH similar to the PDV; 2) the solution must be homogeneous; 3)

intensity of detected adducts must be equal or superior to those observed in basic conditions (heme dissolved in ammonia).[24] Given the insolubility of heme in acidic aqueous media, optimization of these conditions was not straightforward.[39] Recent reports suggest that hemozoin formation may occur at interfaces of aqueous and lipidic regions in the PDV.[38,48] Data from X-ray tomography of the digestive vacuole indicate that while lipid nanospheres are important for hematin (heme crystals formed *in vitro* are similar to hemozoin but are called hematin) nucleation, crystal growth may occur in the aqueous phase.[49,50] The PDV biological lipids mixture being solid at room temperature (it is liquid at 37°C), n-octanol has been suggested as a more convenient biomimetic model than glycerides mixture.[51,52] N-octanol is an amphiphilic molecule with a hydrophobic aliphatic tail of medium length and a hydrophilic polar head which is smaller than the glycerol ester functional groups of mono- and diglyceride lipids.[53] Accordingly, solubility of water is lower in n-octanol than in a glycerides mixture, but it is still sufficient for hydrogen bond formation and hematin crystals formation.[48] On the other hand, the lower solubility of heme at low pH is due to the intermolecular hydrogen bonds between propionic residues. The formation of these bonds requires protonation of the carboxyl groups, which strongly increases at lower pH.[38] Value of pH may indirectly affect the formation of π- π complexes by modifying the physicochemical characteristics of the molecules involved.[22] The lower the pH, the higher the amount of dimers and the lower the solubility. Citric buffer saturated octanol (CBSO) was found to properly solubilize heme.[25,37] Octanol mimics the lipid nanospheres, while solubilized citric buffer imitates the acidic environment of the parasite's digestive vacuole.[14,37] We used a modified CBSO for this work, bringing its pH to 5.2. Additional pH at 4.8 and 5 were tested. Modifications of the buffer were made by substituting citric acid by formic acid (final pH 5.2) or ammonia (final pH 10) with the goal of improving solubility of hemin and compounds in the octanol mixture as well as resolution and intensity of adducts signals. Nevertheless none of these options was as effective as citric acid.

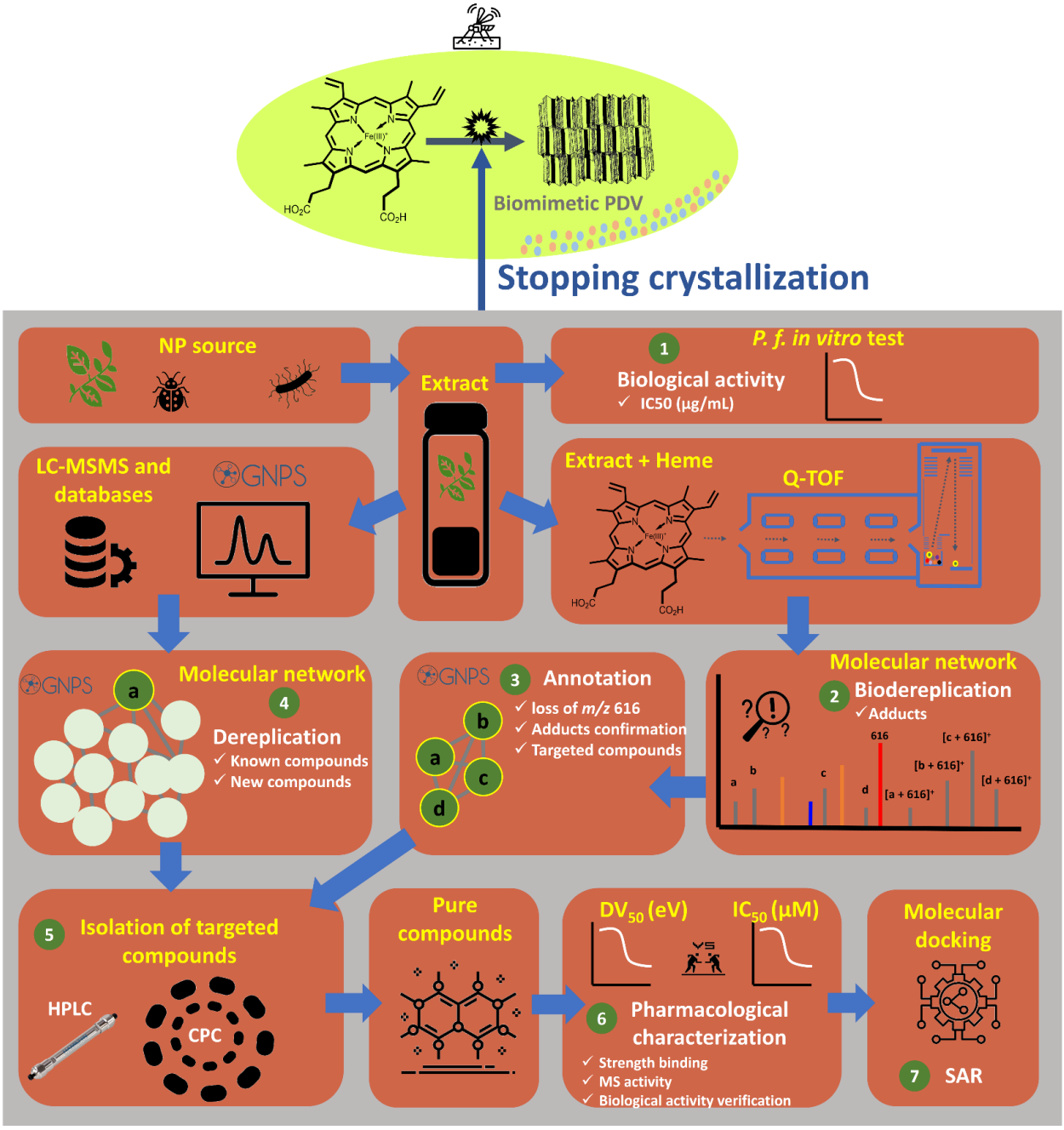

Figure 1. Biodereplication workflow as a wall building to stop heme crystallization. NP source = Natural products source; *P.f.* = *Plasmodium falciparum*.

A mix of eight antimalarial drugs or an alkaloid extract of *C. pubescens* were used to optimize and validate the first part of the workflow. Due to the peculiar nature of the solution composed by octanol, DMSO and water, parameters of the ionization source were optimized to allow evaporation, ionization and to decrease background noise. Temperature and gas flow were slightly increased compared to usual conditions, to 325 °C and 11 L/min, respectively. To ease the formation of

micellar interface, we added a small concentration of detergent Tween 20, previously developed to initiate heme crystallization.[54] MS spectra (**Figure 2-A**) showed apparent adducts formed by non-covalent binding of antimalarial drugs incubated with heme-Fe(III) in an acidic medium. Deciphering such signals to detect adducts can be performed by several ways. The simplest way is to compare 1) the spectrum from the extract and 2) the spectrum of the mixture of extract with heme, and visually detect whether new ions of *m/z* > 616 (heme) appear in the second case. A program script could be designed to analyze data and automatically detect such discrepancies. Another way is to use a triple quadrupole instrument in precursor ion mode. If the second quadrupole is set to detect *m/z* 616, any adduct analyzed in the first quadrupole and able to produce heme as a fragment upon dissociation should be pointed out. Unfortunately, such instruments do not provide high *m/z* accuracy and are not able to give any information about the molecular formulas of unknown compounds. On the contrary, a Q-ToF instrument is providing high accuracy readings but is strictly speaking not able to work in precursor ion mode. Indeed, it needs to gather ions in a "pulse" before flight time measurement, and thus cancels the "separation in time" of precursor ions by the two first quadrupoles. Although a Q-ToF instrument is able to indicate when a target fragment ion is produced but is unable to indicate to which precursor it correlates. This limitation can be artificially minimized when running a chromatographic separation, but since in our case the injection is in infusion mode, we cannot use the Q-ToF in precursor ion mode. We therefore propose to use the molecular networking (MN) approach to take advantage of Q-ToF instruments accuracy and still be able to automatically detect heme adducts. In such an approach, a network is computerized by the GNPS platform[10] to detect ions producing heme fragment upon dissociation. In such an analysis, parameters can be set up so as every species producing *m/z* 616 as a fragment is plotted as a node in a same network cluster. Other heme fragments were identified at *m/z* 557 and 498 corresponding to the loss of the first and second carboxymethyl groups, [heme – $CH_2COOH]^+$ and [heme – $(CH_2COOH)_2]^+$ ions respectively.[55] Nodes in a cluster are connected following their cosine values. Cosine value approaches 1 when fragmentations routes are very similar.[11] Every drug of the mix of antimalarial drugs

was detected in the same cluster, although most of these drugs do not belong to the same chemical family. In the other hand, heme adduct cluster from alkaloid extract (**Figure 2-B**) showed all known compounds detected by LCMS (see SI5). In this case these compounds belong to the same sub-family of quinoline alkaloids, some of the adducts (*e.g. m/z* 956) resulting possibly from the binding of heme with quinoline artifacts.[56,57]

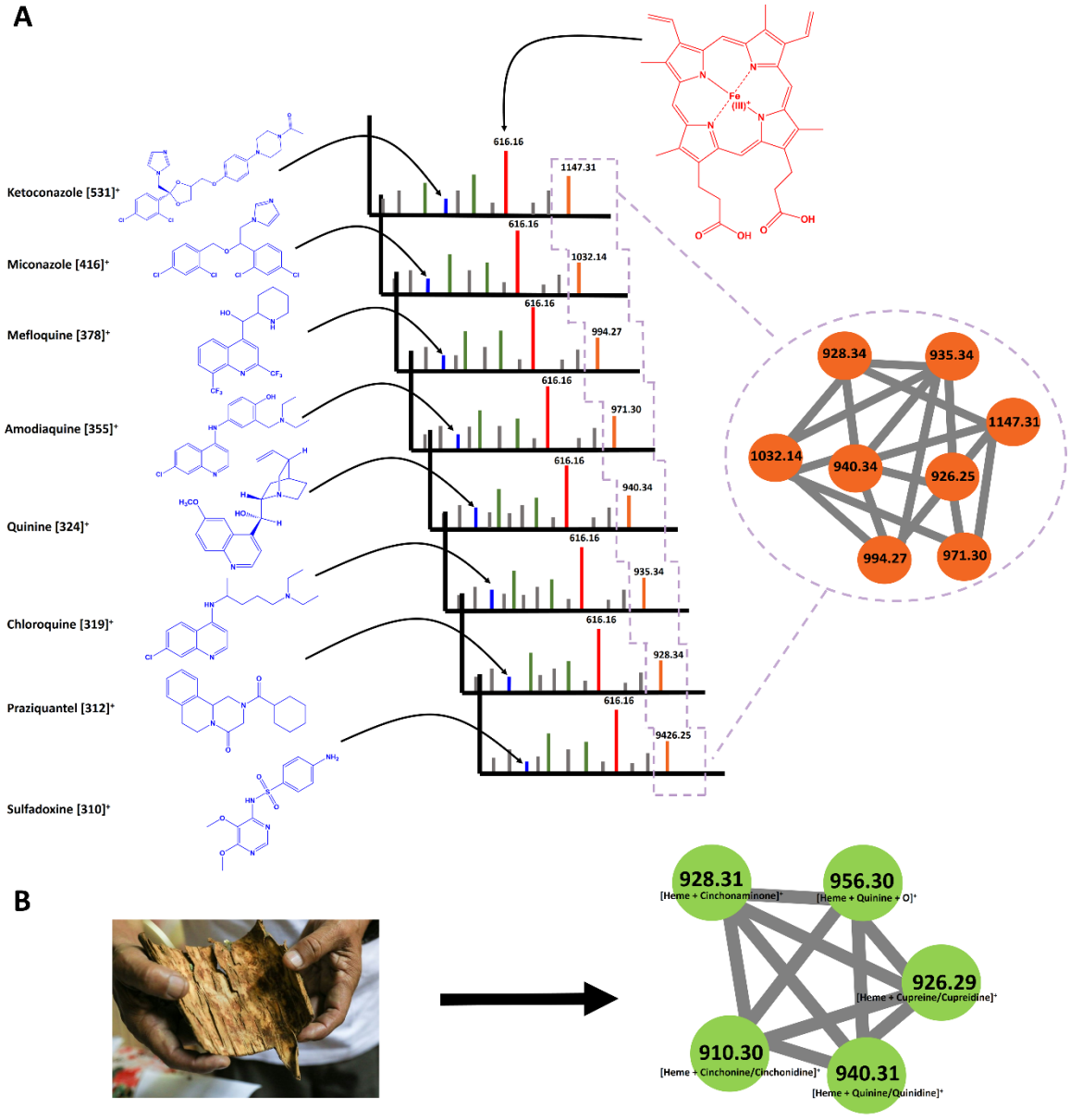

Figure 2 Visualization by MS and molecular networking of heme adducts for main antimalarial drugs (**A**) and alkaloid extract from *Cinchona pubescens.* (**B**).

Our example of biodereplication workflow was carried on *Piper coruscans* leaves extract. In **Figure 3-A**, for the ethanolic extract from *P. coruscans*, analysis by MS heme-test showed five *m/z* of interest: 914.2938, 900.2814, 886.5327 and 871.5579. In the same spectrum, adducts of heme were also identified. Network of MSMS for targeted adducts is showed in **Figure 3-B**. Nodes within the cluster are connected with satisfactory cosine values in the range of 0.7 to 0.96. Adduct at *m/z* 871.55 (molecular formula $C_{16}H_{17}NO_2$) corresponded to trace amounts of a minor compound in the ethanolic extract at *m/z* 256.13 $[M+H]^+$ (**Figure 3C1 and C2**). Observed adducts at *m/z* 914.28 (molecular formula C_{18} $H_{18}O_4$), 900.28 (molecular formula $C_{17}H_{16}O_4$) and 886.53 (molecular formula $C_{16}H_{14}O_4$) were expected to correspond to compounds in the extract at *m/z* 299, 285, and 271 respectively. Looking for these compounds in the LC-MS data revealed several isobaric species in the ethanolic extract (**Figure 3C3-C5**). On MN clustering (**Figure 3-B**) it was not possible to obtain several nodes of same *m/z* for the different isomers. Although recent developments have shown how to visualize by MN clustering isomers, this is only possible if isomers have different retention time[58] using data processing software's to mine data (*e.g.* MZmine).[59] This might to be the case for the isomers detected on the LC-MS data (**Figure 3C1-C5**), nevertheless this is not possible due to the fact that injection is done by infusion mode, with all analytes being injected in the source simultaneously. We do not know reports so far of dereplication by MN of extracts by direct injection. Our aim in this work is the rapid visualization of non-covalent binds without chromatography separation. Also, we did not use a chromatographic column to avoid adducts dissociation during elution. Injection after rapid mixing and short incubation guarantees the persistence of non-covalent bounds even of low strength. These isobaric species were distinguished by molecular networking principally in ethyl acetate extract, except for the non-polar compounds (**1**, **4**, and **5**). The molecular network also allows to determine that compounds **6**, **2**, **3**, **7**, **8**, **9** are likely belonging to the same phytochemical family (*i.e.* flavonoids), whereas **10** (cinnamoyl derivative) and **11** (alkamide) belong to different, less represented phytochemical families (see SI6). Along with these targeted compounds one known untargeted compound was isolated

(**12**). All molecular structures are presented in **Figure 3D**.

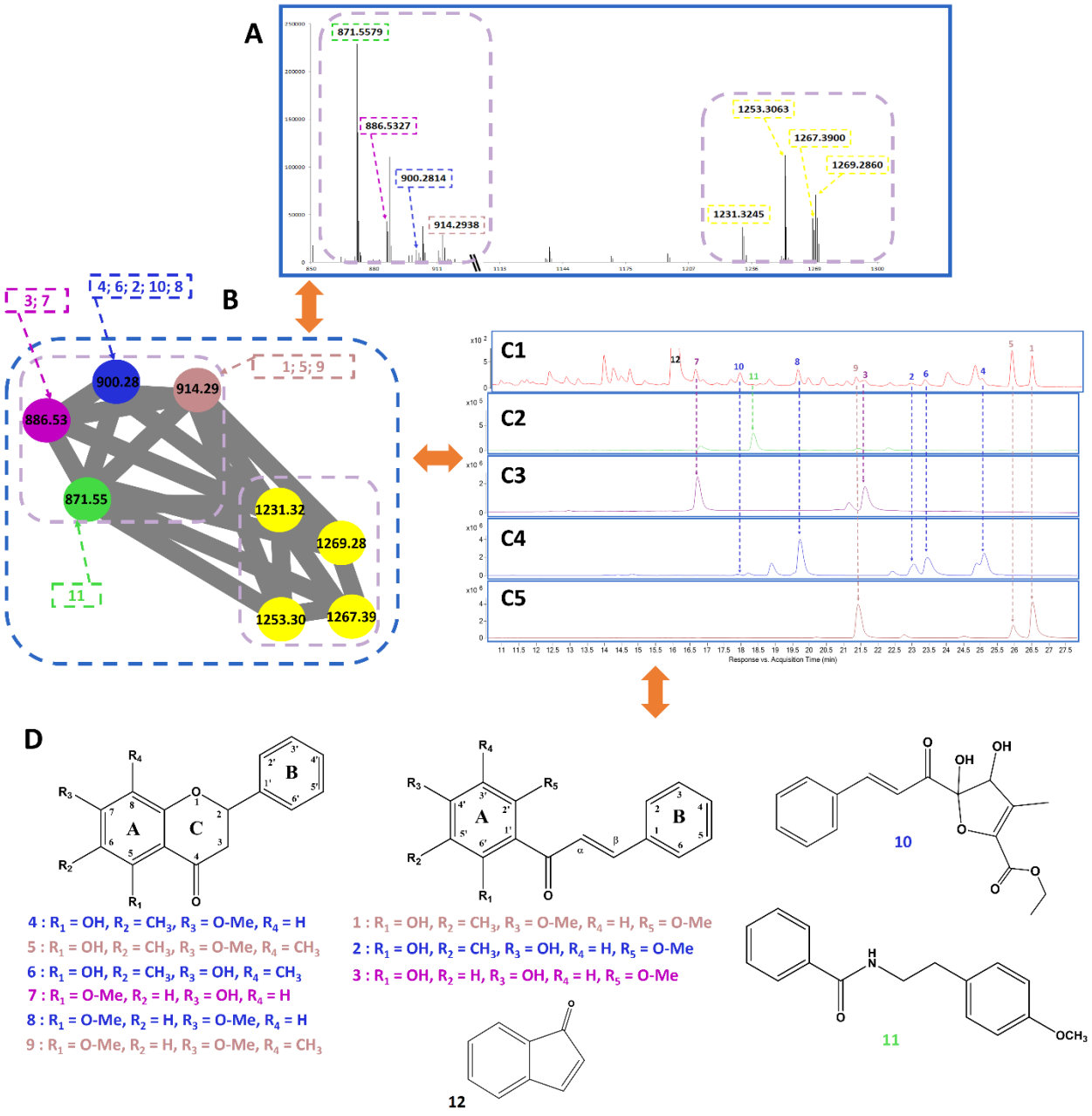

Figure 3. Biodereplication workflow from *P. coruscans* leaves extract. A) MS spectrum of heme-extract mixture. B) Network showing targeted adducts grouped in the same cluster. C1) LC-DAD (280 nm) of ethanolic extract from *P. coruscans*, with corresponding extracted spectra of C2) *m/z* 256, C3) *m/z* 271, C4) *m/z* 285, C5) *m/z* 299. D) Targeted molecular structures isolated.

Once *m/z* of target compounds were identified, we performed a mass-guided isolation. We targeted these molecules by CPC using a mixture of five solvents specifically optimized for this purpose. The choice of a solvent system is guided by the solubility of the analytes as well as their partition coefficient. In the preliminary optimization step, a rational selection of suitable stationary and mobile phases is essential.[60] This fivefold mixture of solvents (heptane/ethyl acetate/butanol/methanol/water) was selected as it provided good factor of retention and selectivity for the targeted molecules, namely, a partition coefficient of nearly 1 for the targeted analytes and different from 1 for other analytes. Two solvents systems were designed, the first system suited to non-polar compounds with heptane/ethyl acetate/butanol/methanol/water (12:14:14:23:37) and another system suited to moderately polar compounds with heptane/ethyl acetate/butanol/methanol/water (8:16:16:18:42) by increasing proportions of ethyl acetate and butanol in the organic phase. Non-polar compounds **1**, **4**, and **5**, were isolated by CPC as can be seen in the CPC fractograms (See SI7). For polar compounds, LC-MS analysis of both phases of several biphasic systems allowed to determine that the solvents system heptane/ethyl acetate/butanol/methanol/water (20:10:10:30:30) showed a satisfactory selectivity targeted on flavonoids compounds like flavanones or chalcones. This system is a variant from the Oka range in which hexane was replaced by heptane.[60] The use of this system allowed to obtain compound **1**, **4** and **5** in only one step (injection of ethyl acetate fraction in the CPC system, collection of pure compounds). Other compounds required a polishing step by preparative HPLC.

Targeted compounds isolated from *P. coruscans* displaying *m/z* 299 (compounds **1**, **5**, **9**), 285 (compounds **4**, **6**, **2**, **10**, **8**), 271 (compounds **3**, **7**) and 256 (compound **11**) were identified as known molecules (**Figure 3-D**), which corresponded to flavonoids family except compounds **10** (ethyl 5-cinnamoyl-4,5-dihydroxy-3-methyl-4,5-dihydrofuran-2-carboxylate) and **11** (*N*-benzoyltyramine methyl ether). Compounds **4-9** are flavanones, compounds **1-3** are chalcones. All structures were described previously in the literature. Compound **10** is a new compound, described as a product of degradation in MS source (see SI1). *Piper* species are aromatic plants used in the

traditional medicine in tropical and subtropical regions. Alkaloids/amides as piperine (neuroprotective)[61], piplartine (anticancer proprieties and antiparasitic against *Schistosoma mansoni*)[62,63], aduncamide (antibacterial against *Bacillus subtilis* and *Micrococcus luteus*)[64] or benzoic acid derivatives (antiplasmodial against *P. falciparum*)[65] are only a few examples of the active compounds which validate these uses of *Piper* species. Isolated compounds from genus *Piper* may include also propenylphenols, lignans, neolignans, terpenes, steroids, kawapyrones, piperolides, flavones, chalcones and dihydrochalcones.[66]

Antiplasmodial activity of *P. coruscans* ethanolic extract was promising (IC_{50} = 1.36 µg/mL).[29] Chalcones **1** (aurentiacin) and **3** (cardamonin) showed the best antiplasmodial activity with IC_{50} = 2.25 and 5.5 µM, respectively. Aurentiacin **1** has the lowest cytotoxicity on fibroblasts and the highest selectivity index, suggesting it is the most interesting structure (**Table 1**). Considering their low DV_{50} of 5.15 and 5.60 eV, their antiplasmodial activity is probably not related to a heme binding mechanism, as other authors also suggested.[67] Cardamonin **3** was reported to have significant activity against *Trypanosoma brucei* (IC_{50} = 0.49 µg/mL), a parasite which is not relying on hemoglobin for its metabolism.[68] Studies also showed that cardamonin binds with high affinity to site II of HSA (human serum albumin).[69] Chalcones are abundant in edible plants and are considered to be precursors of flavonoids and isoflavonoids. The presence of a double bond conjugated with the carbonyl is believed to be responsible for the biological activities of chalcones, as the removal of the double bound inactivates them.[70] The antimalarial activity of chalcones has a great interest. Several natural and synthetic chalcones have been described to possess antimalarial effect.[71] Their antimalarial activity is supposed to be a result of a Michael addition of cellular nucleophilic sites to the activated double bond.[72] Indeed, the Michael acceptor site of chalcones can readily form covalent bonds with the sulfhydryl of cysteines or other thiols to obtain a Michael adduct which may play an important role in biological activities of chalcones.[73] Covalent heme-chalcone adducts by Michael addition pathway have not been not reported so far. Nevertheless asymmetric Michael addition of nitroalkanes to chalcones was reported.[71] Licochalcone A is an example of a chalcone inhibiting *in vitro* growth of both

chloroquine-sensitive (3D7) and chloroquine-resistant (Dd2) strains of *P. falciparum*. It was shown to have multiple targets in *P. falciparum* mitochondria. It inhibited ubiquinol cytochrome *c* reductase (bc1 complex) and succinate ubiquinone reductase (complex II).[67] It is known that chalcones bearing a -Cl group in position 4 of ring A, and -OCH_3 (position-3) and -allyloxy (position-4) on ring B are active against 3D7 *P. falciparum* with average values of IC_{50} of 2.5 µM.[74,75]

Table 1. Antiplasmodial activity, cytotoxicity and dissociation voltage of isolated compounds.

Family derivatives	Compounds	*m/z* $[M + H]^+$	Adducts expected with heme-Fe (III)	3D7 sensitive strain SYBR green IC_{50} (µM)	AB943 Primary human dermal fibroblast CC_{50} (µM)	Selectivity index CC_{50}/IC_{50}	DV_{50} (eV)	cLogP (ACD/ChemSketch)
chalcones	**1**	299	915	2.25	68.5	30.4	5.15	4.47
	2	285	900	51	>100	1.9	5.93	4.08
	3	271	886	5.5	58	10.5	5.60	3.62
flavanones	**4**	285	900	60	>100	< 1	NA	4.57
	5	299	915	33.2	23	< 1	NA	5.03
	6	285	900	71	>100	1.4	NA	4.85
	7	271	886	72	>100	1.4	8.40	3.71
	8	285	900	78	>100	1.3	8.68	3.40
	9	299	915	85	>100	1.2	7.68	3.86
cinnamoyl derivative	**10**	285	900	>100	>100	1	NA	2.44
alkylamide	**11**	256	871	>100	>100	1	9.45	2.79
indanone	**12**	131	746*	>100	>100	1	NA	2.21
Crude extract				1.36 µg/ml	37.5 µg/ml	27.6	NT	-
Quinolein	CQ	320	935	0.04 ± 3.25	NT	NT	14.27	3.93
Sesquiterpene lactone	ART	283	898 (heme-Fe(II)	0.004 ± 0.1[76]	NT	NT	15.93	3.11

NT= not tested; NA= no adduct; CQ= Chloroquine; ART= Artemisinin. *Adduct not detected.

All the isolated flavanones (**4-9**) showed a moderate antiplasmodial activity, ranging from 85 to 33 µM (**Table 1**). This activity can be partly explained by their cytotoxicity, as their selectivity index are very low. On the other hand, DV_{50} values for the compounds were in accordance with this moderate activity, as these compounds would not bind or bind only loosely (DV_{50} in the range 8-9) while chloroquine had a DV_{50} above 14 (**Figure 4**).

It should be highlighted that a non-covalent bis-adduct was observed for quinine [(2heme-Fe(III) – H)+quinine]$^+$ at *m/z* 1556.539 (see SI8). Docking studies on hemozoin-quinoline drugs also reported such sandwich adduct with quinine and chloroquine.[77] Nevertheless in our experiment, this adduct was not deconvoluted by molecular networking into a heme-binding compound. This may be explained by the fact that these adducts are dissociated at very low collision energies. At last, we showed that under acidic and reductive conditions, several artemisinin-heme-Fe(II) covalent adducts are detected at *m/z* 838, 898, 1180 (see SI9). The adduct at *m/z* 838 [heme + artemisinin -CH_2-COOH + H]$^+$ was shown to be of covalent nature by MSMS analyses, as it is reported in the literature.[41] Reductive activation of endoperoxide by Fe(II) heme produces the homolytic cleavage of the endoperoxide bond and the subsequent formation of artemisinin-heme adduct able to alkylate heme or other proteins.[24] The DV_{50} value of the artemisinin covalent adduct is similar of that of chloroquine but the profile of the stability curve is not sigmoidal. This is due to the fact that in such a case the observed effect is not a dissociation but an actual fragmentation with covalent bound breakage. Adducts at *m/z* 898 [heme + artemisinin]$^+$ and 1180 [heme + 2 artemisinin]$^+$ were identified for the first time by MS as being non covalent adducts as they would dissociate very quickly and have a DV_{50} < 2 (data not shown).

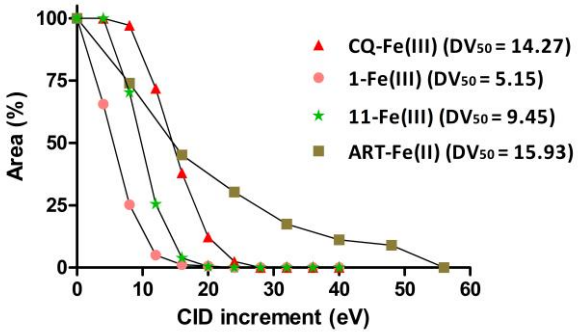

Figure 4. Dissociation curves for the more significant compounds isolated from *Piper coruscans* compared with chloroquine (CQ) and artemisinin (ART).

CONCLUSIONS

Crystallization of heme is the principal pathway used by *Plasmodium* to detoxify hemoglobin digestion by-products. Interruption of this process still remains of interest as it does not lead to resistance *per se*. Our biodereplication methodology contributes to the rapid and efficient detection of potentially antimalarial molecules in complex mixtures. In addition, this method does not require cultures of parasites and can be implemented in a high-throughput format. The direct infusion mode allows us to have the information of adducts from the extract in 3 minutes. The automatic mixing realized in the autosampler in a 384-well plates for the analyses MS and MSMS allows to process 384 extracts in less than 20 hours. Furthermore a miniaturized format accounts for minimal reagent consumption**.** Molecular networking is a bold and efficient technique of visualizing the non-covalent binding in complex extracts. It can be applied to decipher raw data obtained by MSMS analyses. The approach has been applied to a *Piper* extract, pointing out chalcones as the main compounds responsible for the antiplasmodial activity. The biodereplication method allows a rapid, economic and robust technique to identify possible active compounds with the aim to economize time, money and effort.

ASSOCIATED CONTENT

(SI) Supporting Information

The Supporting Information will be available free.

AUTHOR INFORMATION

Corresponding Author

*E-mail: alexandre.maciuk@u-psud.fr

Notes

The authors declare no competing financial interest

ACKNOWLEDGEMENTS

The authors thank the Consejo de Ciencia y Tecnología del Perú (CONCYTEC) (Council for science and technology of Peru) (299 - 2014 -FONDECYT) for the Ph.D. scholarship (PGVO). We also appreciate the contribution of A. Fox, M. Beniddir (Université Paris Sud), B. Cabanillas, K. Mejia, E. Rengifo(Instituto de Investigaciones de la Amazonia Peruana), J.-M. Nuzillard and A. Martinez (Université de Reims Champagne-Ardenne).

REFERENCES

(1) Phillips, M.; Burrows, J.; Christine, M.; van Huijsduijnen, R.; Van Voorhis, W.; Timothy, W. Malaria. *Nat. Rev. Dis. Primer* **2017**, *3*, 17051. https://doi.org/doi:10.1038/nrdp.2017.50.

(2) WHO. Malaria, Fact Sheet. 2016.

(3) Cui, L.; Su, X. Discovery, Mechanisms of Action and Combination Therapy of Artemisinin. *Expert Rev. Anti Infect. Ther.* **2009**, *7* (8), 999–1013. https://doi.org/10.1586/eri.09.68.

(4) WHO. Global Technical Strategy for Malaria 2016–2030. 2015.

(5) Cui, L.; Mharakurwa, S.; Ndiaye, D.; Rathod, P. K.; Rosenthal, P. J. Antimalarial Drug Resistance: Literature Review and Activities and Findings of the ICEMR Network. *Am. J. Trop. Med. Hyg.* **2015**, *93* (3 Suppl), 57–68. https://doi.org/10.4269/ajtmh.15-0007.

(6) Olliaro, P. Drug Resistance Hampers Our Capacity to Roll Back Malaria. *Clin. Infect. Dis.* **2005**, *41* (Supplement_4), S247–S257. https://doi.org/10.1086/430785.

(7) Hubert, J.; Nuzillard, J.-M.; Renault, J.-H. Dereplication Strategies in Natural Product Research: How Many Tools and Methodologies behind the Same Concept? *Phytochem. Rev.* **2017**, *16* (1), 55–95. https://doi.org/10.1007/s11101-015-9448-7.

(8) Beutler, J. A.; Alvarado, A. B.; Schaufelberger, D. E.; Andrews, P.; McCloud, T. G. Dereplication of Phorbol Bioactives: *Lyngbya majuscula* and *Croton cuneatus*. *J. Nat. Prod.* **1990**, *53* (4), 867–874. https://doi.org/10.1021/np50070a014.

(9) Garg, N.; Kapono, C. A.; Lim, Y. W.; Koyama, N.; Vermeij, M. J. A.; Conrad, D.; Rohwer, F.; Dorrestein, P. C. Mass Spectral Similarity for Untargeted Metabolomics Data Analysis of Complex Mixtures. *Int. J. Mass Spectrom.* **2015**, *377* (Supplement C), 719–727. https://doi.org/10.1016/j.ijms.2014.06.005.

(10) Yang, J. Y.; Sanchez, L. M.; Rath, C. M.; Liu, X.; Boudreau, P. D.; Bruns, N.; Glukhov, E.; Wodtke, A.; de Felicio, R.; Fenner, A.; et al. Molecular Networking as a Dereplication Strategy. *J. Nat. Prod.* **2013**, *76* (9), 1686–1699. https://doi.org/10.1021/np400413s.

(11) Wan, K. X.; Vidavsky, I.; Gross, M. L. Comparing Similar Spectra: From Similarity Index to Spectral Contrast Angle. *J. Am. Soc. Mass Spectrom.* **2002**, *13* (1), 85–88. https://doi.org/10.1016/S1044-0305(01)00327-0.

(12) Pashynska, V. A.; Van den Heuvel, H.; Claeys, M.; Kosevich, M. V. Characterization of Noncovalent Complexes of Antimalarial Agents of the Artemisinin-Type and FE(III)-Heme by Electrospray Mass Spectrometry and Collisional Activation Tandem Mass Spectrometry. *J. Am. Soc. Mass Spectrom.* **2004**, *15* (8), 1181–1190. https://doi.org/10.1016/j.jasms.2004.04.030.

(13) Gligorijevic, B.; Bennett, T.; McAllister, R.; Urbach, J. S.; Roepe, P. D. Spinning Disk Confocal Microscopy of Live, Intraerythrocytic Malarial Parasites. 2. Altered Vacuolar Volume Regulation in Drug Resistant Malaria. *Biochemistry* **2006**, *45* (41), 12411–12423. https://doi.org/10.1021/bi0610348.

(14) Hayward, R.; Saliba, K. J.; Kirk, K. The PH of the Digestive Vacuole of *Plasmodium falciparum* Is Not Associated with Chloroquine Resistance. *J. Cell Sci.* **2006**, *119* (6), 1016. https://doi.org/10.1242/jcs.02795.

(15) Wunderlich, J.; Rohrbach, P.; Dalton, J. P. The Malaria Digestive Vacuole. *Front. Biosci. Sch. Ed.* **2012**, *4*, 1424–1448.

(16) Olliaro, P. L.; Goldberg, D. E. The *Plasmodium* Digestive Vacuole: Metabolic Headquarters and Choice Drug Target. *Parasitol. Today* **1995**, *11* (8), 294–297. https://doi.org/10.1016/0169-4758(95)80042-5.

(17) Wu, B.; Novelli, J.; Foster, J.; Vaisvila, R.; Conway, L.; Ingram, J.; Ganatra, M.; Rao, A. U.; Hamza, I.; Slatko, B. The Heme

Biosynthetic Pathway of the Obligate Wolbachia Endosymbiont of *Brugia malayi* as a Potential Anti-Filarial Drug Target. *PLoS Negl. Trop. Dis.* **2009**, *3* (7), e475. https://doi.org/10.1371/journal.pntd.0000475.

(18) Oliveira, M. F.; d'Avila, J. C. P.; Tempone, A. J.; Correâ Soares, J. B. R.; Rumjanek, F. D.; Ferreira-Pereira, A.; Ferreira, S. T.; Oliveira, P. L. Inhibition of Heme Aggregation by Chloroquine Reduces *Schistosoma mansoni* Infection. *J. Infect. Dis.* **2004**, *190* (4), 843–852. https://doi.org/10.1086/422759.

(19) Tekwani, B. L.; Walker, L. A. Targeting the Hemozoin Synthesis Pathway for New Antimalarial Drug Discovery: Technologies for in Vitro Beta-Hematin Formation Assay. *Comb. Chem. High Throughput Screen.* **2005**, *8* (1), 63–79. https://doi.org/10.2174/1386207053328101.

(20) Buller, R.; Peterson, M. L.; Almarsson, Ö.; Leiserowitz, L. Quinoline Binding Site on Malaria Pigment Crystal: A Rational Pathway for Antimalaria Drug Design. *Cryst. Growth Des.* **2002**, *2* (6), 553–562. https://doi.org/10.1021/cg025550i.

(21) Kappe, S. H. I.; Vaughan, A. M.; Boddey, J. A.; Cowman, A. F. That Was Then But This Is Now: Malaria Research in the Time of an Eradication Agenda. *Science* **2010**, *328* (5980), 862. https://doi.org/10.1126/science.1184785.

(22) Parapini, S.; Basilico, N.; Pasini, E.; Egan, T. J.; Olliaro, P.; Taramelli, D.; Monti, D. Standardization of the Physicochemical Parameters to Assess *in Vitro* the β-Hematin Inhibitory Activity of Antimalarial Drugs. *Exp. Parasitol.* **2000**, *96* (4), 249–256. https://doi.org/10.1006/expr.2000.4583.

(23) Adams, P. A.; Berman, P. A. M.; Egan, T. J.; Marsh, P. J.; Silver, J. The Iron Environment in Heme and Heme-Antimalarial Complexes of Pharmacological Interest. *J. Inorg. Biochem.* **1996**, *63* (1), 69–77. https://doi.org/10.1016/0162-0134(95)00212-X.

(24) Muñoz-Durango, K.; Maciuk, A.; Harfouche, A.; Torijano-Gutiérrez, S.; Jullian, J.-C.; Quintin, J.; Spelman, K.; Mouray, E.; Grellier, P.; Figadère, B. Detection, Characterization, and Screening of Heme-Binding Molecules by Mass Spectrometry for Malaria Drug Discovery. *Anal. Chem.* **2012**, *84* (7), 3324–3329. https://doi.org/10.1021/ac300065t.

(25) Olafson, K. N.; Ketchum, M. A.; Rimer, J. D.; Vekilov, P. G. Mechanisms of Hematin Crystallization and Inhibition by the Antimalarial Drug Chloroquine. *Proc. Natl. Acad. Sci. U. S. A.* **2015**, *112* (16), 4946–4951. https://doi.org/10.1073/pnas.1501023112.

(26) Wang, M.; Carver, J. J.; Phelan, V. V.; Sanchez, L. M.; Garg, N.; Peng, Y.; Nguyen, D. D.; Watrous, J.; Kapono, C. A.; Luzzatto-Knaan, T.; et al. Sharing and Community Curation of Mass Spectrometry Data with Global Natural Products Social Molecular Networking. *Nat. Biotechnol.* **2016**, *34*, 828. https://doi.org/doi: 10.1038/nbt.3597.

(27) Trager, W.; Jensen, J. B. Human Malaria Parasites in Continuous Culture. *Science* **1976**, *193* (4254), 673–675. https://doi.org/10.1126/science.781840.

(28) Lambros, C.; Vanderberg, J. P. Synchronization of *Plasmodium falciparum* Erythrocytic Stages in Culture. *J. Parasitol.* **1979**, *65* (3), 418–420.

(29) Vásquez-Ocmín, P.; Cojean, S.; Rengifo, E.; Suyyagh-Albouz, S.; Amasifuen Guerra, C. A.; Pomel, S.; Cabanillas, B.; Mejía, K.; Loiseau, P. M.; Figadère, B.; et al. Antiprotozoal Activity of Medicinal Plants Used by Iquitos-Nauta Road Communities in Loreto (Peru). *J. Ethnopharmacol.* **2018**, *210*, 372–385. https://doi.org/10.1016/j.jep.2017.08.039.

(30) Komlaga, G.; Cojean, S.; Dickson, R. A.; Beniddir, M. A.; Suyyagh-Albouz, S.; Mensah, M. L. K.; Agyare, C.; Champy, P.; Loiseau, P. M. Antiplasmodial Activity of Selected Medicinal Plants Used to Treat Malaria in Ghana. *Parasitol. Res.* **2016**,

115 (8), 3185–3195. https://doi.org/10.1007/s00436-016-5080-8.

(31) Bounaadja, L.; Schmitt, M.; Albrecht, S.; Mouray, E.; Tarnus, C.; Florent, I. Selective Inhibition of PfA-M1, over PfA-M17, by an Amino-Benzosuberone Derivative Blocks Malaria Parasites Development *in Vitro* and *in Vivo*. *Malar. J.* **2017**, *16* (1), 382. https://doi.org/10.1186/s12936-017-2032-4.

(32) Feixiong Cheng; Weihua Li; Guixia Liu and Yun Tang. In Silico ADMET Prediction: Recent Advances, Current Challenges and Future Trends. *Curr. Top. Med. Chem.* **2013**, *13* (11), 1273–1289. https://doi.org/10.2174/15680266113139990033.

(33) Trott, O.; Olson, A. J. AutoDock Vina: Improving the Speed and Accuracy of Docking with a New Scoring Function, Efficient Optimization, and Multithreading. *J. Comput. Chem.* **2009**, *31* (2), 455–461. https://doi.org/10.1002/jcc.21334.

(34) Pettersen, E. F.; Goddard, T. D.; Huang, C. C.; Couch, G. S.; Greenblatt, D. M.; Meng, E. C.; Ferrin, T. E. UCSF Chimera--a Visualization System for Exploratory Research and Analysis. *J. Comput. Chem.* **2004**, *25* (13), 1605–1612. https://doi.org/10.1002/jcc.20084.

(35) Ponka, P. Cell Biology of Heme. *Am. J. Med. Sci.* **1999**, *318* (4), 241–256. https://doi.org/10.1016/S0002-9629(15)40628-7.

(36) White, K. A.; Marletta, M. A. Nitric Oxide Synthase Is a Cytochrome P-450 Type Hemoprotein. *Biochemistry* **1992**, *31* (29), 6627–6631. https://doi.org/10.1021/bi00144a001.

(37) Olafson, K. N.; Rimer, J. D.; Vekilov, P. G. Growth of Large Hematin Crystals in Biomimetic Solutions. *Cryst. Growth Des.* **2014**, *14* (5), 2123–2127. https://doi.org/10.1021/cg5002682.

(38) Ketchum, M. A.; Olafson, K. N.; Petrova, E. V.; Rimer, J. D.; Vekilov, P. G. Hematin Crystallization from Aqueous and Organic Solvents. *J. Chem. Phys.* **2013**, *139* (12), 121911. https://doi.org/10.1063/1.4816106.

(39) Stiebler, R.; Hoang, A. N.; Egan, T. J.; Wright, D. W.; Oliveira, M. F. Increase on the Initial Soluble Heme Levels in Acidic Conditions Is an Important Mechanism for Spontaneous Heme Crystallization *In Vitro*. *PLOS ONE* **2010**, *5* (9), e12694. https://doi.org/10.1371/journal.pone.0012694.

(40) Basilico, N.; Pagani, E.; Monti, D.; Olliaro, P.; Taramelli, D. A Microtitre-Based Method for Measuring the Haem Polymerization Inhibitory Activity (HPIA) of Antimalarial Drugs. *J. Antimicrob. Chemother.* **1998**, *42* (1), 55–60. https://doi.org/10.1093/jac/42.1.55.

(41) Robert, A.; Coppel, Y.; Meunier, B. NMR Characterization of Covalent Adducts Obtained by Alkylation of Heme with the Antimalarial Drug Artemisinin. *Protag. Chem. Helmut Sigel* **2002**, *339*, 488–496. https://doi.org/10.1016/S0020-1693(02)00940-4.

(42) Ortiz, S.; Dali-Yahia, K.; Vasquez-Ocmin, P.; Grougnet, R.; Grellier, P.; Michel, S.; Maciuk, A.; Boutefnouchet, S. Heme-Binding Activity of Methoxyflavones from *Pentzia monodiana* Maire (Asteraceae). *Fitoterapia* **2017**, *118*, 1–5. https://doi.org/10.1016/j.fitote.2017.01.012.

(43) Loo, J. A. Studying Noncovalent Protein Complexes by Electrospray Ionization Mass Spectrometry. *Mass Spectrom. Rev.* **1997**, *16* (1), 1–23. https://doi.org/10.1002/(SICI)1098-2787(1997)16:1<1::AID-MAS1>3.0.CO;2-L.

(44) Gupta, R.; Hamdan, S. M.; Dixon, N. E.; Sheil, M. M.; Beck, J. L. Application of Electrospray Ionization Mass Spectrometry to Study the Hydrophobic Interaction between the ε and θ Subunits of DNA Polymerase III. *Protein Sci. Publ. Protein Soc.* **2004**, *13* (11), 2878–2887. https://doi.org/10.1110/ps.04889604.

(45) Veenstra, T. D. Electrospray Ionization Mass Spectrometry in the Study of Biomolecular Non-Covalent Interactions. *Biophys. Chem.* **1999**, *79* (2), 63–79.

https://doi.org/10.1016/S0301-4622(99)00037-X.
(46) Wright, A. D.; Wang, H.; Gurrath, M.; König, G. M.; Kocak, G.; Neumann, G.; Loria, P.; Foley, M.; Tilley, L. Inhibition of Heme Detoxification Processes Underlies the Antimalarial Activity of Terpene Isonitrile Compounds from Marine Sponges. *J. Med. Chem.* **2001**, *44* (6), 873–885. https://doi.org/10.1021/jm0010724.
(47) Krieg, R.; Jortzik, E.; Goetz, A.-A.; Blandin, S.; Wittlin, S.; Elhabiri, M.; Rahbari, M.; Nuryyeva, S.; Voigt, K.; Dahse, H.-M.; et al. Arylmethylamino Steroids as Antiparasitic Agents. *Nat. Commun.* **2017**, *8*, 14478. https://doi.org/10.1038/ncomms14478.
(48) Vekilov, P. G.; Rimer, J. D.; Olafson, K. N.; Ketchum, M. A. Lipid or Aqueous Medium for Hematin Crystallization? *CrystEngComm* **2015**, *17* (41), 7790–7800. https://doi.org/10.1039/C5CE01178G.
(49) Kapishnikov, S.; Berthing, T.; Hviid, L.; Dierolf, M.; Menzel, A.; Pfeiffer, F.; Als-Nielsen, J.; Leiserowitz, L. Aligned Hemozoin Crystals in Curved Clusters in Malarial Red Blood Cells Revealed by Nanoprobe X-Ray Fe Fluorescence and Diffraction. *Proc. Natl. Acad. Sci. U. S. A.* **2012**, *109* (28), 11184–11187. https://doi.org/10.1073/pnas.1118134109.
(50) Kapishnikov, S.; Weiner, A.; Shimoni, E.; Guttmann, P.; Schneider, G.; Dahan-Pasternak, N.; Dzikowski, R.; Leiserowitz, L.; Elbaum, M. Oriented Nucleation of Hemozoin at the Digestive Vacuole Membrane in *Plasmodium falciparum*. *Proc. Natl. Acad. Sci.* **2012**, *109* (28), 11188–11193. https://doi.org/10.1073/pnas.1118120109.
(51) Egan, T. J. Haemozoin Formation. *Mol. Biochem. Parasitol.* **2008**, *157* (2), 127–136. https://doi.org/10.1016/j.molbiopara.2007.11.005.
(52) Egan, T. J. Recent Advances in Understanding the Mechanism of Hemozoin (Malaria Pigment) Formation. *J. Inorg. Biochem.* **2008**, *102* (5), 1288–1299. https://doi.org/10.1016/j.jinorgbio.2007.12.004.
(53) Sangster, J. *Octanol-Water Partition Coefficients: Fundamentals and Physical Chemistry*; Wiley: England, 1997; Vol. 2.
(54) Huy, N. T.; Uyen, D. T.; Maeda, A.; Trang, D. T. X.; Oida, T.; Harada, S.; Kamei, K. Simple Colorimetric Inhibition Assay of Heme Crystallization for High-Throughput Screening of Antimalarial Compounds. *Antimicrob. Agents Chemother.* **2007**, *51* (1), 350–353. https://doi.org/10.1128/AAC.00985-06.
(55) Charkin, O. P.; Klimenko, N. M.; Nguyen, P. T.; Charkin, D. O.; Mebel, A. M.; Lin, S. H.; Wang, Y.-S.; Wei, S.-C.; Chang, H.-C. Fragmentation of Heme and Hemin+ with Sequential Loss of Carboxymethyl Groups: A DFT and Mass-Spectrometry Study. *Chem. Phys. Lett.* **2005**, *415* (4), 362–369. https://doi.org/10.1016/j.cplett.2005.09.036.
(56) Ateacha, D. N.; Koch, U.; Engelhard, C. Direct Analysis of Alkaloids in Natural Cinchona Bark and Commercial Extracts Using Time-of-Flight Secondary Ion Mass Spectrometry. *Anal. Methods* **2018**, *10* (9), 950–958. https://doi.org/10.1039/C7AY02822A.
(57) Shibuya, H.; Kitamura, C.; Maehara, S.; Nagahata, M.; Winarno, H.; Simanjuntak, P.; Kim, H.-S.; Wataya, Y.; Ohashi, K. Transformation of Cinchona Alkaloids into 1-N-Oxide Derivatives by Endophytic Xylaria Sp. Isolated from *Cinchona pubescens*. *Chem. Pharm. Bull. (Tokyo)* **2003**, *51* (1), 71–74. https://doi.org/10.1248/cpb.51.71.
(58) Olivon, F.; Grelier, G.; Roussi, F.; Litaudon, M.; Touboul, D. MZmine 2 Data-Preprocessing To Enhance Molecular Networking Reliability. *Anal. Chem.* **2017**. https://doi.org/10.1021/acs.analchem.7b01563.
(59) Pluskal, T.; Castillo, S.; Villar-Briones, A.; Oresic, M. MZmine 2: Modular Framework for Processing, Visualizing, and Analyzing Mass Spectrometry-Based

Molecular Profile Data. *BMC Bioinformatics* **2010**, *11*, 395–395. https://doi.org/10.1186/1471-2105-11-395.

(60) Berthod, A. *Comprehensive Analytical Chemistry Volume XXXVIII: Countercurrent Chromatography - The Support-Free Liquid Stationary Phase*; Elsevier, 2002; Vol. 38.

(61) Hua, S.; Liu, J.; Zhang, Y.; Li, J.; Zhang, X.; Dong, L.; Zhao, Y.; Fu, X. Piperine as a Neuroprotective Functional Component in Rats with Cerebral Ischemic Injury. *Food Sci. Nutr.* **2019**, *0* (0). https://doi.org/10.1002/fsn3.1185.

(62) Raja Mazlan, R. N. A.; Rukayadi, Y.; Maulidiani, M.; Ismail, I. S. Solvent Extraction and Identification of Active Anticariogenic Metabolites in *Piper cubeba* L. through ^{1}H-NMR-Based Metabolomics Approach. *Mol. Basel Switz.* **2018**, *23* (7), 1730. https://doi.org/10.3390/molecules23071730.

(63) Campelo, Y.; Ombredane, A.; Vasconcelos, A. G.; Albuquerque, L.; Moreira, D. C.; Plácido, A.; Rocha, J.; Hilarion Fokoue, H.; Yamaguchi, L.; Mafud, A.; et al. Structure Activity Relationship of Piplartine and Synthetic Analogues against *Schistosoma mansoni* and Cytotoxicity to Mammalian Cells. *Int. J. Mol. Sci.* **2018**, *19* (6), 1802. https://doi.org/10.3390/ijms19061802.

(64) Orjala, J.; Wright, A. D.; Rali, T.; Sticher, O. Aduncamide, a Cytotoxic and Antibacterial b-Phenylethylamine-Derived Amide from *Piper aduncum*. *Nat. Prod. Lett.* **1993**, *2* (3), 231–236. https://doi.org/10.1080/10575639308043814.

(65) Braga, F. G.; Bouzada, M. L. M.; Fabri, R. L.; de O. Matos, M.; Moreira, F. O.; Scio, E.; Coimbra, E. S. Antileishmanial and Antifungal Activity of Plants Used in Traditional Medicine in Brazil. *J. Ethnopharmacol.* **2007**, *111* (2), 396–402. https://doi.org/10.1016/j.jep.2006.12.006.

(66) Parmar, V. S.; Jain, S. C.; Bisht, K. S.; Jain, R.; Taneja, P.; Jha, A.; Tyagi, O. D.; Prasad, A. K.; Wengel, J.; Olsen, C. E.; et al. Phytochemistry of the Genus *Piper*. *Int. J. Plant Biochem. Mol. Biol.* **1997**, *46* (4), 597–673. https://doi.org/10.1016/S0031-9422(97)00328-2.

(67) Mi-Ichi, F.; Miyadera, H.; Kobayashi, T.; Takamiya, S.; Waki, S.; Iwata, S.; Shibata, S.; Kita, K. Parasite Mitochondria as a Target of Chemotherapy: Inhibitory Effect of Licochalcone A on the *Plasmodium falciparum* Respiratory Chain. *Ann. N. Y. Acad. Sci.* **2005**, *1056* (1), 46–54. https://doi.org/10.1196/annals.1352.037.

(68) Xiao, H.; Rao Ravu, R.; Tekwani, B. L.; Li, W.; Liu, W.-B.; Jacob, M. R.; Khan, S. I.; Cai, X.; Peng, C.-Y.; Khan, I. A.; et al. Biological Evaluation of Phytoconstituents from *Polygonum hydropiper*. *Nat. Prod. Res.* **2017**, *31* (17), 2053–2057. https://doi.org/10.1080/14786419.2016.1269094.

(69) He, W.; Li, Y.; Liu, J.; Hu, Z.; Chen, X. Specific Interaction of Chalcone-Protein: Cardamonin Binding Site II on the Human Serum Albumin Molecule. *Biopolymers* **2005**, *79* (1), 48–57. https://doi.org/10.1002/bip.20328.

(70) Gomes, M. N.; Muratov, E. N.; Pereira, M.; Peixoto, J. C.; Rosseto, L. P.; Cravo, P. V. L.; Andrade, C. H.; Neves, B. J. Chalcone Derivatives: Promising Starting Points for Drug Design. *Mol. Basel Switz.* **2017**, *22* (8), 1210. https://doi.org/10.3390/molecules22081210.

(71) Zhuang, C.; Zhang, W.; Sheng, C.; Zhang, W.; Xing, C.; Miao, Z. Chalcone: A Privileged Structure in Medicinal Chemistry. *Chem. Rev.* **2017**, *117* (12), 7762–7810. https://doi.org/10.1021/acs.chemrev.7b00020.

(72) Ram, V. J.; Saxena, A. S.; Srivastava, S.; Chandra, S. Oxygenated Chalcones and Bischalcones as Potential Antimalarial Agents. *Bioorg. Med. Chem. Lett.* **2000**, *10* (19), 2159–2161.

https://doi.org/10.1016/S0960-894X(00)00409-1.
(73) Gan, F.-F.; Kaminska, K. K.; Yang, H.; Liew, C.-Y.; Leow, P.-C.; So, C.-L.; Tu, L. N.; Roy, A.; Yap, C.-W.; Kang, T.-S.; et al. Identification of Michael Acceptor-Centric Pharmacophores with Substituents That Yield Strong Thioredoxin Reductase Inhibitory Character Correlated to Antiproliferative Activity. *Antioxid. Redox Signal.* **2013**, *19* (11), 1149–1165. https://doi.org/10.1089/ars.2012.4909.
(74) Sharma, N.; Mohanakrishnan, D.; Sharma, U. K.; Kumar, R.; Richa; Sinha, A. K.; Sahal, D. Design, Economical Synthesis and Antiplasmodial Evaluation of Vanillin Derived Allylated Chalcones and Their Marked Synergism with Artemisinin against Chloroquine Resistant Strains of *Plasmodium falciparum*. *Eur. J. Med. Chem.* **2014**, *79*, 350–368. https://doi.org/10.1016/j.ejmech.2014.03.079.
(75) Singh, P.; Anand, A.; Kumar, V. Recent Developments in Biological Activities of Chalcones: A Mini Review. *Eur. J. Med. Chem.* **2014**, *85*, 758–777. https://doi.org/10.1016/j.ejmech.2014.08.033.
(76) Lobo, L.; Cabral, L. I. L.; Sena, M. I.; Guerreiro, B.; Rodrigues, A. S.; de Andrade-Neto, V. F.; Cristiano, M. L. S.; Nogueira, F. New Endoperoxides Highly Active *in Vivo* and *in Vitro* against Artemisinin-Resistant *Plasmodium falciparum*. *Malar. J.* **2018**, *17*, 145. https://doi.org/10.1186/s12936-018-2281-x.
(77) Weissbuch, I.; Leiserowitz, L. Interplay Between Malaria, Crystalline Hemozoin Formation, and Antimalarial Drug Action and Design. *Chem. Rev.* **2008**, *108* (11), 4899–4914. https://doi.org/10.1021/cr078274t.